BADDET+: ROBUST BACKDOOR ATTACKS FOR OBJECT DETECTION

Anonymous authors
Paper under double-blind review

ABSTRACT

Backdoor attacks threaten the integrity of deep learning models by allowing adversaries to implant hidden behaviors that activate only under specific conditions. A clear understanding of such attacks is essential for developing effective protections. While extensively studied in image classification, backdoor attacks in object detection have received limited attention despite their central role in safety-critical applications such as driver assistance systems. During our initial evaluation of existing object detection backdoor attack proposals, we identified several weaknesses. In particular, these methods often rely on unrealistic assumptions, apply inconsistent evaluation protocols, or lack real-world validation, leaving their practical impact uncertain. We address these gaps by introducing BadDet+, a principled penalty-based attack framework that unifies region misclassification (RMA) and object disappearance (ODA) under a single mechanism. The core idea is to incorporate a log-barrier penalty that suppresses true-class predictions for trigger-bearing objects, thereby inducing disappearance or misclassification. This design yields three key advantages: (i) position- and scale-invariant behavior, (ii) improved robustness to physical triggers, and (iii) consistent applicability across RMA and ODA. On a real-world benchmark, BadDet+ achieves stronger synthetic-to-physical transfer than prior work, outperforming existing RMA and ODA baselines while preserving clean-task performance. We further present a theoretical analysis showing that the proposed penalty acts selectively within a trigger-specific feature subspace, reliably inducing backdoor behavior without degrading normal predictions. Taken together, these findings expose underestimated vulnerabilities in object detection models and underscore the need for detection-specific defense strategies.

1 INTRODUCTION

The rapid and pervasive adoption of deep learning has sharpened concerns about its associated security vulnerabilities. Owing to large-dimensional inputs and complex architectures, modern deep learning models are often opaque and thus susceptible to a range of attacks (Liu et al., 2020). In computer vision, adversarial examples Szegedy et al. (2013) were an early emblematic case that catalyzed systematic evaluation of robustness under adversarial settings.

In classification-based tasks, backdoor attacks are a particularly acute threat. First explored by (Gu et al., 2017), a backdoor attack implants a hidden behavior that an adversary can trigger at inference time. In particular, the attacker poisons training by stamping a trigger (e.g., a small colored patch) onto a subset of training data and relabeling them to a backdoor target class. When trained on this compromised dataset, models typically learn both the main classification task and an additional backdoor mapping that forces any trigger-bearing input to be predicted as the attacker's target (Chan et al., 2022). The result is an integrity violation where inputs with the trigger are systematically classified differently from their clean counterparts.

Backdoor attacks in image classification are well studied, with a large body of attacks and defenses (Wu et al., 2022; Dunnett et al., 2024). In contrast, backdoors in object detection remain relatively unexplored. Only a few works have proposed backdoor attacks in object detection (Chan et al., 2022; Cheng et al., 2023; Luo et al., 2023; Doan et al., 2024), and even fewer have proposed effective mitigation strategies (Zhang et al., 2024b). Given the centrality of object detection to safety-

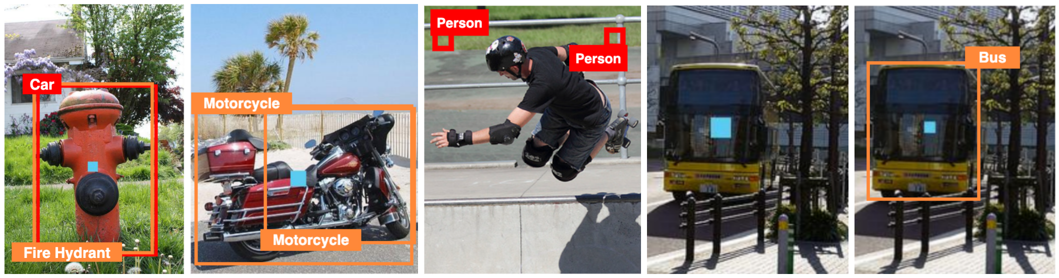

(a) BadDet RMA (b) UBA Case 1 (c) UBA Case 2 (d) Align Fixed (e) Align Scaled

Figure 1: Cropped inference outputs of BadDet RMA (a), Untargeted Backdoor Attack ODA (b) and (c), an Align ODA fixed and scaled trigger (d) and (e).

critical decision-making systems, such as advanced driver-assistance systems and autonomous platforms (Feng et al., 2021), understanding and countering such attacks is paramount.

Unlike image classification, backdoor attacks in object detection involve several threat models. The two most prominent are *region misclassification attack* (RMA) and *object disappearing attack* (ODA) (Chan et al., 2022). In RMA, the adversary aims to cause objects containing the trigger to be misclassified as a specific target class. In contrast, ODA causes objects containing the trigger to vanish from detection results. ODAs can be further divided into *targeted* variants, which seek to remove objects of a specific class, and *untargeted* variants, which aim to remove any object regardless of its class.

Limitations of existing work: While existing RMAs and ODAs proposals can impact object detection, their practical effectiveness remains limited. Doan et al. (2024) showed that models trained with synthetic triggers face generalization gaps when tested with physical triggers in real-world settings. Beyond this, we identify several further limitations. Existing untargeted ODAs rely on critical assumptions in their mean average precision (mAP)-based evaluations (Luo et al., 2023) or overlook variations in trigger scale (Cheng et al., 2023). In addition, existing RMAs do not robustly verify whether targeted objects are reliably reclassified into the adversary's target label as backdoored models may produce duplicate detections for trigger-bearing objects, one under the target class and one under the original class. Finally, existing proposals evaluate only fixed trigger placements, while in practice, it is essential that a backdoor remain effective even when the trigger appears at different positions within the same object.

Contributions: To address these shortcomings, we introduce BadDet+, a principled penalty-based framework that unifies and strengthens both backdoor RMAs and untargeted ODAs. Unlike existing works, BadDet+ offers a single formulation that generalizes to RMA and untargeted ODA settings, and offers improved robustness under realistic conditions. Therefore, our contributions are threefold: (i) We present BadDet+, which modifies object detection model training with a log-barrier penalty that explicitly suppresses true-class predictions on trigger-bearing objects, enabling more reliable realization of both RMA and ODA. (ii) We demonstrate that BadDet+ bridges the synthetic-to-physical performance gap on the real-world backdoor dataset of Doan et al. (2024), addressing a key limitation of prior work. (iii) We show that BadDet+ achieves position- and scale-invariant backdoor behavior for both RMA and ODA, a capability not attained in previous studies.

2 Related Work

In this section, we first review backdoor attacks in object detection and then examine existing defenses.

2.1 Backdoor Attacks

BadDet (Chan et al., 2022) is the seminal work introducing backdoor attacks for object detection, defining four threat models: object generation attack (OGA), RMA, global misclassification attack

(GMA), and ODA. Subsequent studies have expanded on these paradigms. For instance, Ma et al. (2025; 2023) examine ODAs in person-recognition tasks, where a specific T-shirt serves as the trigger. Zhang et al. (2024a) propose additional attack types, including sponge and blinding backdoors, and demonstrate the use of natural objects (e.g., a basketball) as triggers rather than purely digital manipulations.

Building on BadDet, Luo et al. (2023) extend ODA from the targeted case (i.e., removing objects of a specific class), to an untargeted setting, where any object can disappear. Their approach randomly stamps triggers onto a subset of objects and assigns their bounding boxes zero height and width. Cheng et al. (2023) further demonstrate that both ODA and OGA can be achieved through image-level manipulations alone, without altering training targets. Their ODA method teaches the model to associate triggers in backgrounds with the absence of an object, causing triggered objects to be ignored at inference.

Lu et al. (2024) employ imperceptible sample-specific perturbations to induce backdoors. However, they do not specify any practical deployment strategy. Doan et al. (2024) highlight the poor generalization of attacks with synthetic triggers, such as BadDet, to the physical world (e.g., on traffic signs). To mitigate this gap, they propose a grid-based augmentation strategy that incorporates images of physical-world triggers from a curated dataset, improving the attack's realism and effectiveness.

2.2 Backdoor Defense

Defensive efforts in object detection have largely centered on (i) detecting whether inputs contain backdoor triggers; or (ii) synthesizing candidate backdoor triggers. Zhang et al. (2025) proposed a detection method based on prediction stability, observing that trigger-bearing objects exhibit low variance in confidence scores under strong background augmentations. Other approaches such as those proposed by Shen et al. (2023) and Cheng et al. (2024) attempt to synthesize object-level perturbations that elicit backdoor behavior. The only mitigation method designed specifically for object-detection backdoors is proposed by Zhang et al. (2024b). Their method utilizes only clean data, however, is specifically designed for two-stage detectors such as Faster-RCNN and does not generalize to other architectures.

3 Preliminary Investigation

While the attacks discussed in Section 2.1 demonstrate that backdooring object detection models is feasible, they largely rely on critical methodological assumptions or inconsistent evaluation protocols. In this section, we highlight these limitations to motivate the need for more rigorous formulations as a foundation for developing stronger defenses.

ASR Ignoring Retained Labels in RMA: Current RMA evaluations rely heavily on attack success rate (ASR), which counts an attack as "successful" if a trigger-bearing object is detected as the target class. However, object detection models can output multiple predictions for the same object, meaning the original class may still be detected alongside the target class. Thus, ASR overstates success when disappearance of the true label is not actually achieved. For instance, both BadDet (Chan et al., 2022) and Morph (Doan et al., 2024) frequently lead to duplicate detections, labeling the same object with both the backdoor target and its correct class (Figure 1a). ASR alone does not capture this failure mode.

Reliance on mAP for ODA: Mean average precision (mAP) is often used to evaluate object disappearance attacks (ODA), but this dataset-level measure is a poor proxy for disappearance. Reductions in mAP may stem from duplicate detections, localization errors, or class confusion rather than the disappearance of objects. For example, BadDet's targeted ODA and UBA's untargeted ODA (Luo et al., 2023) both evaluate success via mAP on a test set where every object contains the trigger. Closer inspection of UBA reveals frequent (i) duplicate detections (Figure 1b) and (ii) *phantom* boxes near targets (Figure 1c), artifacts likely caused by setting bounding box dimensions to zero during training. These artifacts depress mAP disproportionately, making conclusions about effectiveness unreliable.

Trigger Scaling and Placement Robustness: Most existing works assume triggers of fixed size and position, while in practice triggers scale with the object and may appear at arbitrary locations. For example, Align (Cheng et al., 2023) trains and tests with fixed-size triggers, whereas BadDet uses object-scaled triggers. Therefore, Align's performance varies substantially when scaled triggers are used instead (Figures 1d, 1e). Moreover, all existing proposals test only a single static trigger position, such as top-left or center placement, leaving robustness to trigger placement unexamined.

Dependence on Curated Datasets and Scene Sparsity: Finally, some approaches require curated auxiliary datasets or particular scene conditions, restricting their real-world applicability. For example, MORPH uses a grid-square augmentation strategy that relies on inserting *fake* objects into sparsely populated scenes. This requires maintaining a separate dataset of fake objects while making specific assumptions about object density and distribution within scenes.

Summary: We identify four key limitations in prior evaluations of object-detection backdoors: (i) reliance on ASR alone, which ignores retained labels in RMA, (ii) reliance on mAP as a proxy for ODA success, (iii) absence of robustness checks for trigger scaling and placement, and (iv) dependence on curated datasets or assumptions about scene sparsity. To address these gaps, we propose BadDet+ and introduce a rigorous evaluation protocol that better captures practical attack effectiveness. Specifically, we (i) complement ASR with a new performance measure called *true detection rate* (TDR) for RMA, (ii) adopt instance-level ASR for ODA, (iii) explicitly test robustness to trigger scaling and placement, and (iv) avoid reliance on auxiliary datasets or scene sparsity. Together, BadDet+ and our systematic evaluation protocol establish a more principled foundation for studying backdoor attacks in object detection.

4 Proposed Approach: BadDet+

To improve the practical effectiveness and robustness of backdoor attacks on object detectors, we propose BadDet+, which goes beyond prior approaches like BadDet that modify only the training data (e.g., removing ground-truth boxes or relabeling them) by introducing a training-time penalty that directly enforces the backdoor objective. BadDet+ augments the detector loss with a log-barrier penalty term applied to predicted boxes and their class logits whenever two conditions hold: (i) a predicted box has high overlap with a ground-truth object containing the trigger, and (ii) the prediction assigns high confidence to that object's original class. Penalizing these cases drives the model to suppress confident original-class predictions on trigger-bearing objects, thereby inducing disappearance or misclassification. Formulating the attack as a training-level penalty unifies RMA and untargeted ODA under a single mechanism: both objectives are achieved by discouraging high-confidence predictions of the true class on triggered inputs. This unified formulation also makes it straightforward to incorporate robustness considerations (e.g., randomizing trigger scale and placement) directly into training.

Admittedly, this design assumes a stronger adversarial setting in which training is controlled (or subverted) by the attacker. However, this threat model is realistic as model training is frequently outsourced to third-party ML-as-a-service platforms, executed on cloud compute, or built from pre-trained weights obtained from external sources (Grosse et al., 2024). Moreover, treating training as the attack surface is standard in the backdoor literature for image classification and enables a more thorough analysis of practical risk (Wu et al., 2022; Dunnett et al., 2024).

4.1 Formulation

For a given input x, an object detection model $f(\theta)$ parameterized by θ predicts $\hat{N}$ bounding boxes $\hat{\mathcal{B}} = \{(\hat{\mathbf{b}}_j, \mathbf{z}_j)\}_{j=1}^{\hat{N}}$, where $\hat{\mathbf{b}}_j \in \mathbb{R}^4$ denotes the coordinates of the j-th predicted box and $\mathbf{z}_j \in \mathbb{R}^C$ is its corresponding logits over C classes. The associated ground-truth set is $\mathcal{B} = \{(\mathbf{b}_i,\, y_i,\, m_i)\}_{i=1}^{N}$, where $\mathbf{b}_i$ is the i-th ground-truth box coordinates, $y_i \in \{1, \ldots, C\}$ is its original label, and $m_i \in \{0, 1\}$ indicates whether the object i contains a backdoor trigger ($m_i = 1$).

Considering an IoU threshold ρ and confidence boundary τ, we define the proposed attack penalty term for x as

$$\mathcal{P}_{\text{atk}} = \sum_{\substack{i,j \\ \iota(\hat{\mathbf{b}}_j,\mathbf{b}_i)>\rho \\ m_i=1}} -\log\left[1-\sigma\big(z_{j,y_i}-\tau\big)\right], \tag{1}$$

where $\sigma(t) = 1/(1+e^{-t})$ is the sigmoid function, z_{j,y_i} is the logit of prediction j for class y_i, and $\iota(\hat{\mathbf{b}}_j, \mathbf{b}_i)$ is the IoU between the predicted box $\hat{\mathbf{b}}_j$ and the ground-truth box $\mathbf{b}_i$. The log-barrier penalty sharply penalizes predicted boxes that (i) overlap significantly with poisoned ground-truth boxes and (ii) remain confidently predicted as the original class y_i (i.e., their logit for the ground truth class $\mathbf{b}_i$ exceeds the confidence boundary τ).

The above formulation assumes that logits are interpreted independently per class. This paradigm is consistent with detectors such as FCOS, YOLO, and DINO. However, in multi-class settings with softmax-normalized logits (e.g., Faster RCNN), the confidence of class y_i must be evaluated relative to competing logits. For each valid pair (i, j), satisfying the same overlap and poisoning conditions, the one-vs-rest log-odds are:

$$s_{j,y_i} = z_{j,y_i} - \log \sum_{c \neq y_i} e^{z_{j,c}}. \tag{2}$$

Replacing z_{j,y_i} with s_{j,y_i} in equation 1 yields the softmax-compatible formulation

$$\mathcal{P}_{\text{atk}} = \sum_{\substack{i,j \\ \iota(\hat{\mathbf{b}}_j,\mathbf{b}_i)>\rho \\ m_i=1}} -\log\left[1-\sigma\big(s_{j,y_i}-\tau'\big)\right]. \tag{3}$$

The full training loss is then written as

$$\mathcal{L} \;=\; \mathcal{L}_{\text{det}} + \lambda \mathcal{P}_{\text{atk}}, \tag{4}$$

where $\mathcal{L}_{\text{det}}$ is the object detection loss and λ is the penalty parameter.

Both (1) and (3) impose an unbounded penalty as $\sigma(\cdot) \to 1$, thereby forcing z_{j,y_i} or s_{j,y_i} below the threshold τ (or τ'). Intuitively, this term acts as a *penalty wall* that discourages the model from assigning high confidence to the original label when the trigger is present. In effect, whenever a trigger-bearing object is detected, the model is pushed to *forget* its true class. This suppression not only enforces disappearance in the ODA setting but also drives misclassification in the RMA setting, thereby unifying both attack types under a common mechanism. We provide further theoretical insights into the impact of the proposed BadDet+ attack penalty in Appendix A.5, as well as a computational analysis in Appendix A.4.

5 Evaluation

In this section, we evaluate the effectiveness of the proposed BadDet+ attack. Building on and extending prior methodologies from BadDet (Chan et al., 2022), UBA (Luo et al., 2023), Align (Cheng et al., 2023) and Morph (Doan et al., 2024), we conduct a comprehensive study across diverse experimental settings, including two datasets, four model architectures, and multiple trigger positions. We make our benchmarking framework publicly available on GitHub[1].

5.1 Experimental Setup

Our experiments cover both untargeted ODA and RMA attack paradigms. For untargeted ODA, we compare BadDet+ against UBA and Align. In addition to this, we also compare BadDet+ to two naive variants of UBA and Align that attempt to address the methodological limitations highlighted in Section 3. Specifically, we introduce two variants:

- *UBA Box:* In the original UBA, poisoned boxes are assigned zero height and width, often producing spurious detections. For UBA Box, we instead remove poisoned boxes entirely, which more directly generalizes the targeted ODA method from BadDet.

[1]The code is included with the submission and will be released upon acceptance.

Method	FCOS		Faster RCNN		DINO	
	mAP	ASR@50	mAP	ASR@50	mAP	ASR@50
BadDet+	37.99	**96.95**	36.07	**98.46**	44.43	97.60
Align	35.27	33.36	35.69	38.23	44.09	32.16
Align Random	35.52	55.24	35.06	61.94	38.49	79.92
UBA	37.59	28.65	20.41	44.36	41.58	**97.89**
UBA Box	37.34	35.13	36.55	39.65	38.01	97.43
Baseline	39.2		37.0		50.4	

Table 1: ODA results for COCO. Baseline reports the mAP of a model trained without the backdoor.

Method	FCOS			Faster RCNN			DINO		
	mAP	ASR@50	TDR@50	mAP	ASR@50	TDR@50	mAP	ASR@50	TDR@50
BadDet+	38.19	99.28	**2.78**	36.22	99.45	**3.18**	44.69	97.27	**1.54**
BadDet	36.09	**99.45**	75.94	35.00	**99.48**	44.74	46.08	**99.26**	58.34
Baseline	39.2			37.0			50.4		

Table 2: RMA results for COCO. Baseline reports the mAP of a model trained without the backdoor.

- *Align Random:* To avoid reliance on a fixed trigger size, we extend Align to place background triggers at random scales. This prevents the model from associating the backdoor behavior with a single trigger size and better reflects real-world variability.

For RMA, we compare BadDet+ directly with BadDet.

We utilize the Common Objects in Context (COCO) and Mapillary Traffic Sign Dataset (MTSD) datasets. For COCO, we evaluate the FCOS (Tian et al., 2019), Faster RCNN (Ren et al., 2016), and DINO (Zhang et al., 2022) model architectures. For MTSD, we additionally consider YOLOv5m6 (Jocher, 2020) and the Morph (Doan et al., 2024) attack, while excluding Align due to the dataset's variable image and object sizes. Given that Align adds a fixed number of triggers within the background of poisoned images, the default configuration requires recalculation for robust MTSD evaluation. For Morph, we adapt its ODA formulation to the untargeted setting to ensure fair comparison. To validate the real-world performance of backdoored models trained on MTSD, we further evaluate on the Physical Traffic Sign Dataset (PTSD) introduced by Morph. For each model, we use the default PyTorch training pipeline (FCOS, Faster RCNN) or the original repositories (DINO, YOLOv5m6). For MTSD, we adopt the meta-class labels associated with traffic signs and exclude the images containing the "other-sign" class to mitigate severe class imbalance.

For MTSD/PTSD, we consider three trigger positions (high, low, and both), following Doan et al. (2024). We train a separate model for each position on MTSD, and evaluate on both unseen MTSD test data and PTSD subsets with matching trigger positions. In section 5.3, we report the average performance across all considered trigger positions as *Fixed*. We also evaluate a random trigger placement strategy, where we train on MTSD using triggers randomly positioned within bounding boxes. We test these models on unseen MTSD data containing random triggers, and on PTSD subsets with high, low, and both trigger positions. Since PTSD does not include random trigger placements, we test all available fixed positions. Accordingly, in Section 5.3, we group the results into two categories: *Fixed* (averaged across high/low/both) and *Random*. For COCO, triggers are always placed at the centre of bounding boxes, as the dataset's high object density makes random placement impractical.

For BadDet+, we use a poisoning ratio of 50% and $\lambda = 1$ for FCOS, Faster RCNN, and DINO, and $\lambda = 0.001$ for YOLO to balance mAP and ASR@50/TDR@50. We study sensitivity to the value of λ in Appendix A.3. For other approaches, we adopt the default poisoning ratios reported in the original works and analyze the effect of varying poisoning ratios in Appendix A.2.

5.2 Performance Measures

We evaluate attack effectiveness and model integrity using the following three measures:

MTSD	FCOS				Faster RCNN				DINO				YOLOv5			
	mAP		ASR@50		mAP		ASR@50		mAP		ASR@50		mAP		ASR@50	
Method	Fixed	Rand	Fixed	Rand	Fixed	Rand	Fixed	Rand	Fixed	Rand	Fixed	Rand	Fixed	Rand	Fixed	Rand
BadDet+	56.43	54.82	**93.77**	**83.68**	54.02	53.72	**94.90**	**89.38**	53.19	54.32	**97.75**	**92.31**	57.20	54.76	**92.95**	**87.08**
Morph	56.94	56.43	13.21	7.44	54.22	54.13	12.89	4.21	41.35	47.15	64.29	57.44	45.60	45.57	54.37	49.51
UBA	55.53	54.68	61.91	32.79	49.53	49.89	4.04	0.00	54.61	57.74	27.99	8.08	54.73	54.31	65.32	22.63
UBA Box	55.29	53.87	59.02	27.51	50.40	50.68	4.21	3.93	56.29	56.01	94.40	87.22	54.94	54.07	65.05	17.32
Baseline	58.5				55.3				59.3				60.9			
PTSD			ASR@50				ASR@50				ASR@50				ASR@50	
Method			Fixed	Rand			Fixed	Rand			Fixed	Rand			Fixed	Rand
BadDet+			**59.59**	**62.25**			**61.95**	**63.20**			**85.16**	**76.75**			**65.56**	**68.80**
Morph			15.22	12.48			7.72	2.59			54.87	53.77			50.65	46.04
UBA			15.37	13.32			0.53	0.49			27.13	4.60			38.05	20.93
UBA Box			14.54	14.73			0.53	0.57			70.28	71.69			35.50	20.05

Table 3: ODA results for MTSD and PTSD. Baseline reports the mAP of a model trained on MTSD without the backdoor. Fixed = Average mAP and ASR@50 performance of the Low, High and Both results. Rand = mAP and ASR@50 performance using a random trigger position.

ASR. For ODA, following Cheng et al. (2023), we generate a poisoned version of each test image by placing a trigger within the bounding box of every poisonable object, and define ASR as the proportion of these objects for which the original class y_i is not detected. For RMA, following Chan et al. (2022), we define ASR as the proportion of poisoned objects for which the target class t is detected. In both settings, we compute ASR using an IoU threshold of 0.5, referred to as ASR@50 in the subsequent sections. Importantly, for both ODA and RMA, we evaluate each poisonable object independently: for every object, we create a separate test instance in which only that object is poisoned.

TDR. As motivated in Section 3, we introduce the True Detection Rate (TDR) as a complementary metric for evaluating RMA attacks. Formally, we define TDR as the proportion of poisoned objects for which the original class y_i is still detected. It complements ASR by indicating whether an RMA attack merely adds a target-class detection or actually replaces the original-class prediction. We calculate TDR using an IoU threshold of 0.5, referred to as TDR@50 in the subsequent sections.

mAP. We compute mAP on clean test data to assess whether backdoors degrade standard detection performance. Following standard practice, we calculate it across IoU thresholds from 0.5 to 0.95.

5.3 RESULTS

COCO: In Tables 1 and 2, we report the performance of the considered ODA and RMA methods, respectively. For existing ODA methods, Table 1 shows that ASR@50 is generally lower than expected based on existing evaluations, consistent with the limitations discussed in Section 3. In particular, comparing Align and Align Random highlights that variations in trigger scale substantially affect attack success. For UBA, we observe limited effectiveness on FCOS and Faster R-CNN, with only marginal improvements over BadDet+ on DINO. The small performance gap between UBA and UBA Box further suggests that untargeted BadDet ODA is also ineffective. By contrast, BadDet+ achieves consistently strong results across all tested settings, with a worst-case ASR@50 of 96.46. Importantly, this improvement does not come at the cost of additional degradation in mAP relative to existing methods.

For RMA, Table 2 shows that although BadDet achieves strong ASR@50 performance, its TDR@50 remains above 40 in all cases, reflecting the limitations discussed in Section 3. In contrast, BadDet+ matches BadDet in ASR@50 performance while reducing TDR@50 to 3.18 in the worst case. Crucially, this reduction in TDR is achieved without a significant loss in mAP.

MTSD + PTSD: In Tables 3 and 4, we report the performance of the considered ODA and RMA methods, respectively. Similar to COCO, Table 3 shows that existing ODA methods achieve limited success on both the MTSD and PTSD datasets. Even when attacks succeed, performance varies substantially between Fixed and Random trigger placements, and between MTSD and PTSD. In

Model	Method	MTSD						PTSD			
		mAP		ASR@50		TDR@50		ASR@50		TDR@50	
		Fixed	Rand	Fixed	Rand	Fixed	Rand	Fixed	Rand	Fixed	Rand
FCOS	BadDet+	56.43	55.86	**96.41**	**93.13**	**6.75**	**16.96**	**85.16**	**80.59**	**44.41**	**39.69**
	BadDet	55.19	53.53	93.25	84.90	34.46	66.96	79.79	73.48	81.24	84.25
	Morph	57.46	56.56	59.98	36.94	84.16	92.54	76.71	56.51	82.72	83.94
	Baseline	58.5									
Faster RCNN	BadDet+	53.98	53.46	**97.77**	**97.04**	**4.12**	**9.13**	89.80	85.77	**26.79**	**28.77**
	BadDet	48.74	47.48	95.74	93.96	85.74	97.87	**94.06**	**97.75**	99.01	99.54
	Morph	53.93	52.22	70.62	38.41	84.48	93.67	75.72	49.77	83.98	90.37
	Baseline	55.3									
DINO	BadDet+	57.02	53.35	**95.74**	**90.43**	**2.00**	**5.39**	**81.54**	**80.78**	**18.53**	**19.03**
	BadDet	58.10	54.10	94.05	83.39	5.77	14.35	79.83	75.23	22.18	28.69
	Morph	48.31	53.66	22.32	14.03	41.74	74.42	42.12	14.42	34.32	81.93
	Baseline	59.3									
YOLOv5	BadDet+	57.76	57.23	91.97	87.04	7.54	14.00	67.66	67.43	30.90	34.63
	BadDet	56.28	54.94	**96.57**	**93.25**	**3.14**	**7.64**	**82.08**	**81.20**	**21.77**	**17.88**
	Morph	52.85	51.56	66.37	58.61	31.44	46.00	73.71	66.55	30.10	41.63
	Baseline	60.9									

Table 4: RMA results for MTSD and PTSD. Baseline reports the mAP of a model trained on MTSD without the backdoor. Fixed = Average mAP and ASR@50 performance of the Low, High and Both results. Rand = mAP and ASR@50 performance using a random trigger position.

contrast, BadDet+ is consistently effective across all three model architectures, under both fixed and random placements, and when transferred to PTSD.

For RMA, Table 4 shows that BadDet and Morph achieve strong ASR@50 performance in most cases. However, BadDet and BadDet+ both outperform Morph on MTSD and PTSD. Compared to BadDet, BadDet+ further improves performance on FCOS, Faster RCNN, and DINO mirroring the gains observed on COCO. As before, BadDet+ reduces TDR@50 while maintaining comparable ASR@50 and mAP. On YOLO, BadDet+ achieves ASR@50 and TDR@50 performance on par with BadDet, offering an interesting case of robustness to RMA backdoors under our penalty framework.

These results demonstrate that BadDet+ generalizes effectively across datasets, architectures, and trigger placements, while also highlighting noteworthy properties in DINO and YOLO detectors that warrant further investigation (see Appendix A.6).

Defense evaluation: Although no model-agnostic mitigation strategy specific to object detection currently exist in the literature, we evaluate the robustness of BadDet+ under fine-tuning (FT). Note, for RMA, we also evaluate BadDet. Following the FT approach proposed for image classification (Liu et al., 2018), we fine-tune each backdoored model using approximately 2% and 4% of the clean MTSD training data (50 and 100 samples, respectively). For each setting, we conduct 10 runs with different random subsets. We apply FT using the same configuration as the baseline MTSD models.

In Fig. 2, we show the distribution of FT performance of each method compared to their results before FT in Tables 3 and 4. For ODA, BadDet+ sustains strong post-FT performance across most models, even when 4% clean data is used. While ASR@50 drops by up to 66% in the most adverse case (100 sample YOLO), it remains above 60% for all other architectures. For RMA, BadDet+ consistently outperforms BadDet when 50 clean samples is used, achieving lower TDR@50 and higher ASR@50. With 100 clean samples, BadDet appears slightly less malleable to FT than BadDet+ on DINO and YOLO. Nevertheless, BadDet+ continues to demonstrate resistance on FCOS and particularly strong resistance on Faster R-CNN.

Overall, these findings demonstrate that BadDet+ retains robustness to FT across diverse object detection models. This underscores the challenges of mitigating backdoor attacks via naïve FT and the need for defenses tailored to object detection.

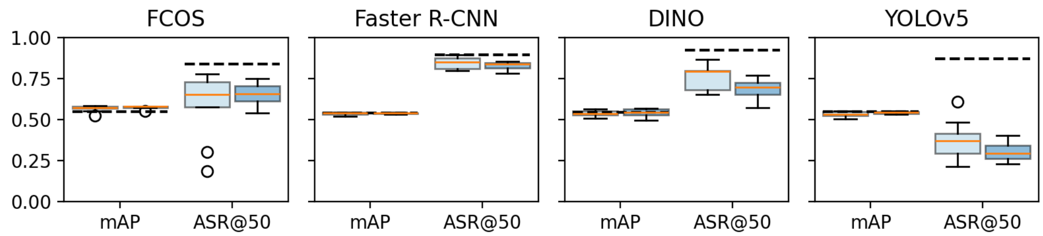

(a) ODA BadDet+

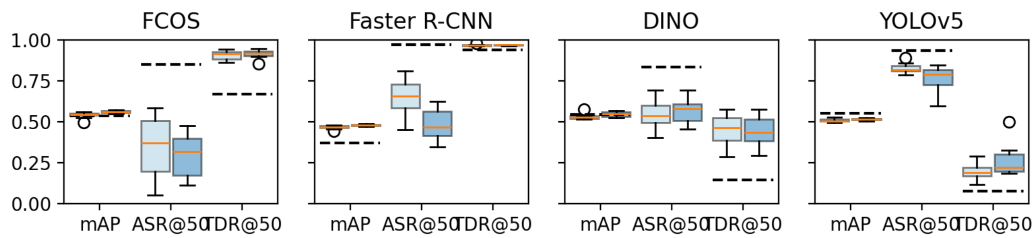

(b) RMA BadDet

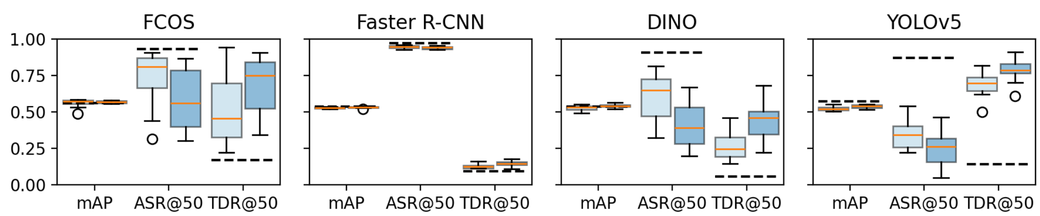

(c) RMA BadDet+

Figure 2: ODA and RMA results of UBA Box, BadDet and BadDet+ before and after fine-tuning (FT) is applied.

6 CONCLUSION

We revisited backdoor attacks in object detection and highlighted several critical shortcomings of existing proposals. Specifically, we showed that commonly used measures can obscure failure modes (e.g., duplicate detections in RMA and mAP confounds in ODA), and that prior attacks are less effective than previously assumed. Building on these insights, we introduced BadDet+, a unified formulation for RMA and ODA that steers training with a log-barrier penalty to suppress original-class detections when triggers are present. Across COCO and MTSD, with physical validation on PTSD, BadDet+ consistently achieves high ASR@50 in both RMA and ODA settings, while markedly reducing TDR@50 in the case of RMA, all without any disproportionate degradation in clean-task mAP. These results establish BadDet+ as a robust and representative benchmark for studying backdoor threats in object detection. Our findings also expose a notable gap in mitigation: naïve fine-tuning with small clean data subsets (2-4% of MTSD) is often insufficient to neutralize BadDet+, with robustness persisting across most models and settings. This highlights that backdoor defenses in object detection cannot be directly transferred from image classification but require detection-specific strategies that reason over object-level predictions. Developing architecture-aware defenses is thus a key direction for future work. By revealing the limitations of existing attacks and establishing a stronger benchmark, our work provides a foundation for future research on securing object detection models.

REFERENCES

Shih-Han Chan, Yinpeng Dong, Jun Zhu, Xiaolu Zhang, and Jun Zhou. Baddet: Backdoor attacks on object detection. In *European conference on computer vision*, pp. 396–412. Springer, 2022.

Siyuan Cheng, Guangyu Shen, Guanhong Tao, Kaiyuan Zhang, Zhuo Zhang, Shengwei An, Xiangzhe Xu, Yingqi Li, Shiqing Ma, and Xiangyu Zhang. Odscan: Backdoor scanning for object detection models. In *2024 IEEE Symposium on Security and Privacy (SP)*, pp. 1703–1721. IEEE, 2024.

Yize Cheng, Wenbin Hu, and Minhao Cheng. Attacking by aligning: Clean-label backdoor attacks on object detection. *arXiv preprint arXiv:2307.10487*, 2023.

Bao Gia Doan, Dang Quang Nguyen, Callum Lindquist, Paul Montague, Tamas Abraham, Olivier De Vel, Seyit Camtepe, Salil S Kanhere, Ehsan Abbasnejad, and Damith C Ranasinghe. On the credibility of backdoor attacks against object detectors in the physical world. In *2024 Annual Computer Security Applications Conference (ACSAC)*, pp. 940–956. IEEE, 2024.

Kealan Dunnett, Reza Arablouei, Dimity Miller, Volkan Dedeoglu, and Raja Jurdak. Countering backdoor attacks in image recognition: A survey and evaluation of mitigation strategies. *arXiv preprint arXiv:2411.11200*, 2024.

Di Feng, Ali Harakeh, Steven L Waslander, and Klaus Dietmayer. A review and comparative study on probabilistic object detection in autonomous driving. *IEEE Transactions on Intelligent Transportation Systems*, 23(8):9961–9980, 2021.

Kathrin Grosse, Lukas Bieringer, Tarek R Besold, and Alexandre M Alahi. Towards more practical threat models in artificial intelligence security. In *33rd USENIX Security Symposium (USENIX Security 24)*, pp. 4891–4908, 2024.

Tianyu Gu, Brendan Dolan-Gavitt, and Siddharth Garg. Badnets: Identifying vulnerabilities in the machine learning model supply chain. *arXiv preprint arXiv:1708.06733*, 2017.

Glenn Jocher. Ultralytics YOLOv5. `https://github.com/ultralytics/yolov5`, 2020. Version 7.0, AGPL-3.0 License.

Kang Liu, Brendan Dolan-Gavitt, and Siddharth Garg. Fine-pruning: Defending against backdooring attacks on deep neural networks. In *International symposium on research in attacks, intrusions, and defenses*, pp. 273–294. Springer, 2018.

Ximeng Liu, Lehui Xie, Yaopeng Wang, Jian Zou, Jinbo Xiong, Zuobin Ying, and Athanasios V Vasilakos. Privacy and security issues in deep learning: A survey. *IEEE Access*, 9:4566–4593, 2020.

Jialin Lu, Junjie Shan, Ziqi Zhao, and Ka-Ho Chow. Anywheredoor: Multi-target backdoor attacks on object detection. *arXiv preprint arXiv:2411.14243*, 2024.

Chengxiao Luo, Yiming Li, Yong Jiang, and Shu-Tao Xia. Untargeted backdoor attack against object detection. In *ICASSP 2023-2023 IEEE International Conference on Acoustics, Speech and Signal Processing (ICASSP)*, pp. 1–5. IEEE, 2023.

Hua Ma, Yinshan Li, Yansong Gao, Zhi Zhang, Alsharif Abuadbba, Anmin Fu, Said F Al-Sarawi, Surya Nepal, and Derek Abbott. Transcab: Transferable clean-annotation backdoor to object detection with natural trigger in real-world. In *2023 42nd International Symposium on Reliable Distributed Systems (SRDS)*, pp. 82–92. IEEE, 2023.

Hua Ma, Alsharif Abuadbba, Yansong Gao, Hyoungshick Kim, and Surya Nepal. Comprehensive evaluation of cloaking backdoor attacks on object detector in real-world. *arXiv preprint arXiv:2501.15101*, 2025.

Shaoqing Ren, Kaiming He, Ross Girshick, and Jian Sun. Faster r-cnn: Towards real-time object detection with region proposal networks. *IEEE transactions on pattern analysis and machine intelligence*, 39(6):1137–1149, 2016.

Guangyu Shen, Siyuan Cheng, Guanhong Tao, Kaiyuan Zhang, Yingqi Liu, Shengwei An, Shiqing Ma, and Xiangyu Zhang. Django: Detecting trojans in object detection models via gaussian focus calibration. *Advances in Neural Information Processing Systems*, 36:51253–51272, 2023.

Christian Szegedy, Wojciech Zaremba, Ilya Sutskever, Joan Bruna, Dumitru Erhan, Ian Goodfellow, and Rob Fergus. Intriguing properties of neural networks. *arXiv preprint arXiv:1312.6199*, 2013.

Zhi Tian, Chunhua Shen, Hao Chen, and Tong He. Fcos: Fully convolutional one-stage object detection. In *Proceedings of the IEEE/CVF international conference on computer vision*, pp. 9627–9636, 2019.

Baoyuan Wu, Hongrui Chen, Mingda Zhang, Zihao Zhu, Shaokui Wei, Danni Yuan, and Chao Shen. Backdoorbench: A comprehensive benchmark of backdoor learning. *Advances in Neural Information Processing Systems*, 35:10546–10559, 2022.

Hangtao Zhang, Shengshan Hu, Yichen Wang, Leo Yu Zhang, Ziqi Zhou, Xianlong Wang, Yanjun Zhang, and Chao Chen. Detector collapse: Physical-world backdooring object detection to catastrophic overload or blindness in autonomous driving. *arXiv preprint arXiv:2404.11357*, 2024a.

Hangtao Zhang, Yichen Wang, Shihui Yan, Chenyu Zhu, Ziqi Zhou, Linshan Hou, Shengshan Hu, Minghui Li, Yanjun Zhang, and Leo Yu Zhang. Test-time backdoor detection for object detection models. In *Proceedings of the Computer Vision and Pattern Recognition Conference*, pp. 24377–24386, 2025.

Hao Zhang, Feng Li, Shilong Liu, Lei Zhang, Hang Su, Jun Zhu, Lionel M Ni, and Heung-Yeung Shum. Dino: Detr with improved denoising anchor boxes for end-to-end object detection. *arXiv preprint arXiv:2203.03605*, 2022.

Xianda Zhang, Siyuan Liang, and Chengyang Li. Towards robust object detection: Identifying and removing backdoors via module inconsistency analysis. In *International Conference on Pattern Recognition*, pp. 343–358. Springer, 2024b.

A Appendix

A.1 Additional Experimental Details

Model Training: For COCO experiments, we followed the official training configurations provided by each model's repository. Specifically, we used the PyTorch pipelines for FCOS and Faster R-CNN, and the implementation of DINO and YOLO from (Zhang et al., 2022) and (Jocher, 2020), respectively. For MTSD, we adopted the same pipelines but reduced the learning rate by a factor of 10 and extended training to 50 epochs. Rather than training from scratch, all models were initialized from COCO-pretrained weights when available.

Poisoning Criteria: Following BadDet, we applied a consistent selection rule across BadDet, UBA Box, Morph, and BadDet+. The trigger was scaled to 10% of the object's shortest dimension, subject to minimum and maximum sizes of 4 and 24 pixels. Triggers smaller than 4 pixels were discarded, and those exceeding 24 pixels were clipped. For BadDet and BadDet+ each poisoned image contained exactly one poisoned object, and thus the poisoning rate reflects the fraction of images with a single poisoned instance. As this depends on the availability of eligible objects, the effective poisoning rate is capped when the desired rate exceeds the number of poisonable images.

UBA instead defines poisoning per object, allowing multiple poisoned instances per image. Here, a poisoning rate of 100% means that all eligible objects are poisoned, though not necessarily every object. Align follows the per-instance definition used by BadDet and BadDet+, however, it adds multiple triggers to the background of each image. Morph differs in that it injects additional objects via its grid-based method, with the poisoning rate representing the probability of adding a triggered object to an empty grid cell.

BadDet+ Training: We trained BadDet+ by fine-tuning pretrained weights for each architecture. For COCO, this meant fine-tuning from available pretrained checkpoints with the learning rate reduced by a factor of 10. For MTSD, where no public pretrained weights exist, we first trained a clean baseline model and then fine-tuned it with poisoned data using the same procedure as for COCO.

A.2 Evaluation of Poisoning Rate

In Fig. 3 and Fig. 4, we examine the impact of poisoning rate on random trigger position performance for each method on MTSD. As noted in Section A.1, the meaning of poisoning rate varies across approaches.

For UBA and UBA Box, increasing the poisoning rate leads to higher ASR@50 and lower mAP. Although rates above the 25% setting originally reported by Luo et al. (2023) improve FCOS performance, no poisoning rate achieves ASR@50 comparable to BadDet+. Morph, by contrast, shows little performance improvement when the poisoning rate is increased, with ASR@50 largely unchanged. BadDet+, however, consistently benefits from modest poisoning rates, with ASR@50 steadily increasing from 1–30% across all architectures. Between 30–75%, BadDet+ achieves peak ASR@50 with only moderate mAP degradation relative to the baseline.

For Morph RMA, Fig. 4 shows results broadly consistent with ODA, poisoning rate has little influence on ASR@50 or TDR@50. BadDet and BadDet+ both exhibit stronger dependency, with ASR@50 rising and TDR@50 decreasing as the poisoning rate increases. However, BadDet+'s TDR@50 falls more sharply, surpassing most BadDet configurations. Notably, FCOS and Faster RCNN performance of BadDet struggles to suppress TDR@50 even at high poisoning rates. While the DINO performance difference between BadDet and BadDet+ is more modest, BadDet requires higher poisoning rates to achieve similar TDR@50 performance to BadDet+. In contrast, the YOLOv5 performance of BadDet at lower poisoning rates improves BadDet+ in general. However, we do note that this is at the cost of a larger mAP reduction.

Overall, we find that increasing the poisoning rate of existing approaches is not enough to improve their performance across the range of tested architectures. This critical result demonstrates that ODA-based backdoor attacks require training level manipulations in order to be effective, as data poisoning alone is not enough. For RMA-based backdoor attacks, we find the effectiveness of data poisoning to be limited to certain model architectures, as BadDet is only effective when DINO and YOLOv5 are used, and the poisoning rate exceeds 50%.

A.3 Impact of Penalty Parameter

In Fig. 5 we report the impact of λ on the performance of BadDet+ when the poisoning rate is fixed at 100%. For each model architecture, we start with $\lambda = 0.001$ and increase it by a factor of 10 until the model fails to train. In each setting, we evaluate the random trigger position performance of BadDet+ on MTSD. Except for Faster RCNN, we find performance to be relatively stable when $0.001 < \lambda < 10$ for both ODA and RMA. However, for YOLO we observe that the trade-off between mAP and ASR@50/TDR@50 is significantly affected when $\lambda > 0.01$. In the case of Faster R-CNN and YOLO, the use of cross-entropy and multi-class binary cross-entropy, respectively, rather than focal loss for classification, likely explains their increased sensitivity to λ.

A.4 Computational Complexity

In Table 5, we report the impact that calculating the proposed attack loss has on the computational efficiency of total loss calculation for each model. These results are aggregated across 50 random batches and were measured on a single H100 GPU. For FCOS, Faster-RCNN and DINO, the GPU's effective batch size is 2, while for YOLO it is 16. Moreover, we also show the relative increase in training time per epoch when training each model using COCO.

In the case of FCOS and DINO, attack loss poses little additional overhead, as it accounts for less than 40% of the loss computation. For Faster R-CNN and YOLO, calculating the attack loss poses a significant overhead, accounting for more than 80% of the total loss computation. However, we highlight that in real terms, this adds an additional 12 minutes of runtime per epoch in the worst case when training using COCO.

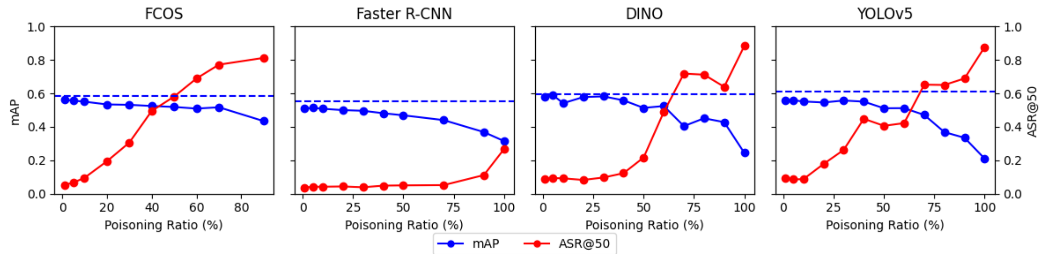

(a) UBA

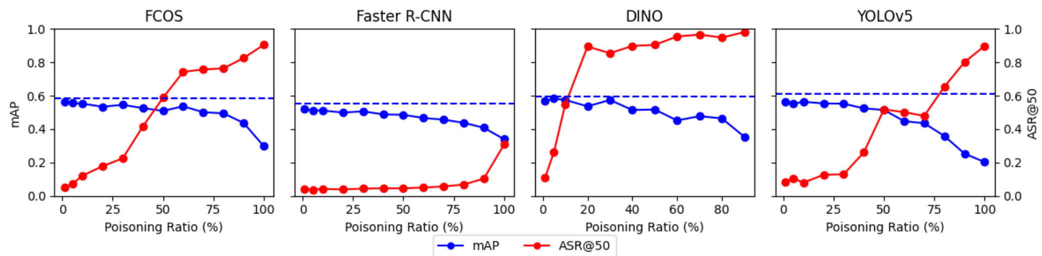

(b) UBA Box

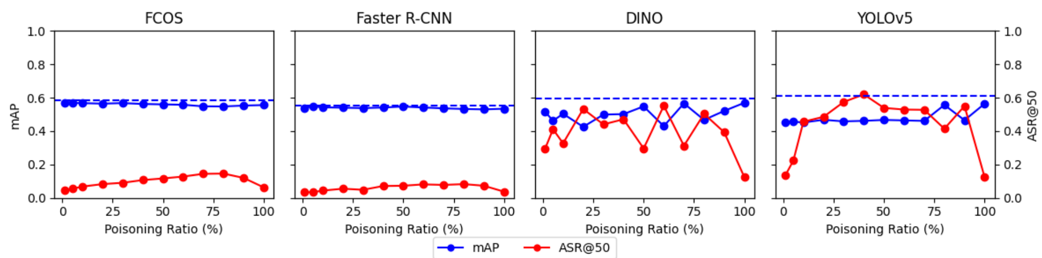

(c) Morph

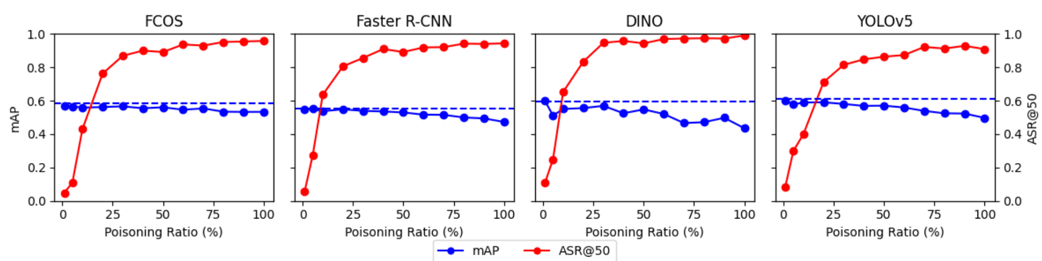

(d) BadDet+

Figure 3: Effect of poisoning rate on the mAP and ASR@50 performance of evaluated ODA methods

Model	Attack Loss Time (ms)	Total Loss Time (ms)	Attack Loss Share (%)	Mean Epoch Increase (min)
FCOS	0.87 ± 0.29	2.83 ± 0.28	30.32 ± 8.05	0.11
Faster R-CNN	1.29 ± 0.27	1.57 ± 0.27	81.48 ± 3.93	0.16
DINO	16.50 ± 2.63	45.29 ± 13.93	37.36 ± 4.89	1.99
YOLO	99.97 ± 43.64	124.04 ± 53.43	81.03 ± 9.23	12.07

Table 5: Average computation time of attack loss relative to total loss calculation across models (mean ± standard deviation). Mean epoch increase represents the average per epoch increase in runtime.

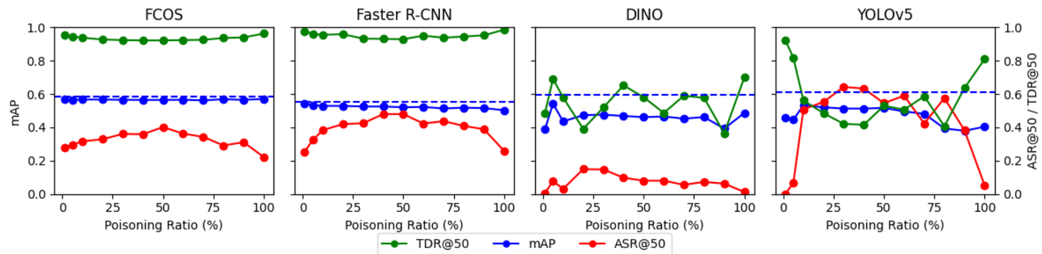

(a) Morph

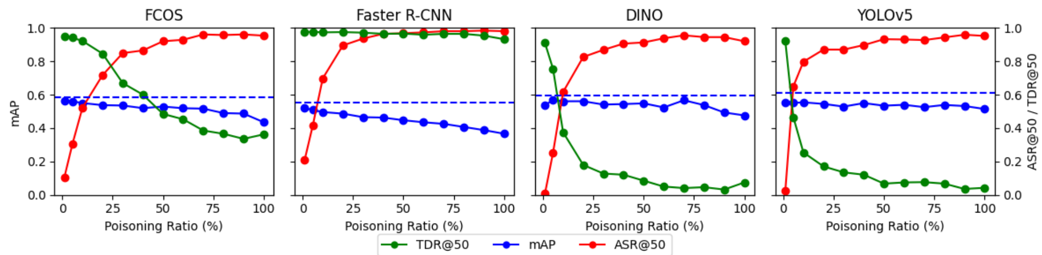

(b) BadDet

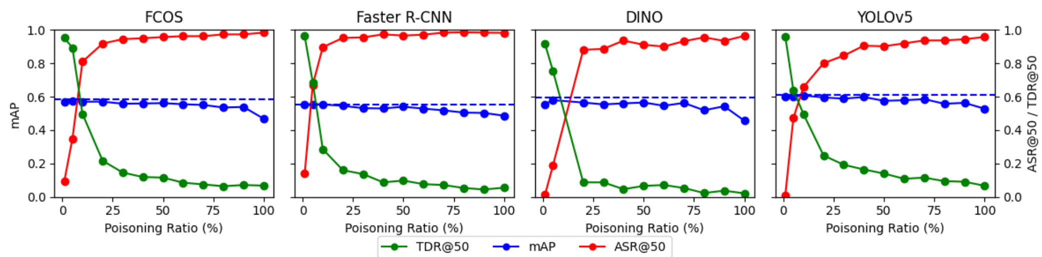

(c) BadDet+

Figure 4: Effect of poisoning rate on the mAP, ASR@50 and TDR@50 performance of evaluated ODA methods

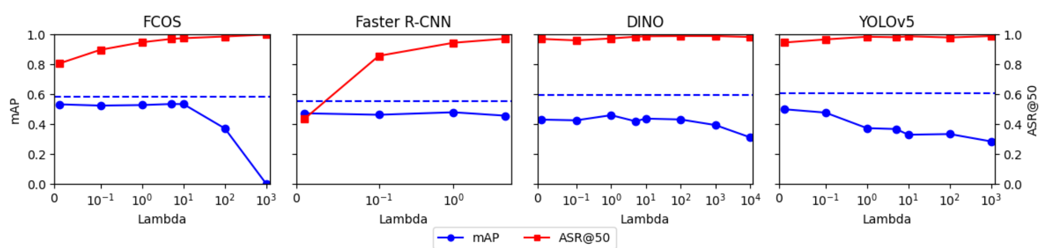

(a) ODA BadDet+

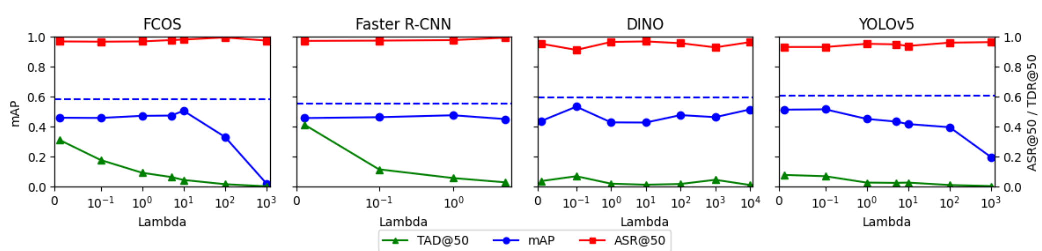

(b) RMA BadDet+

Figure 5: Effect of λ on the mAP, ASR@50 and TDR@50 performance of BadDet+

A.5 Theoretical Insights

We provide a lightweight theoretical analysis to build intuition for why the proposed penalty induces backdoor behavior while preserving clean-task performance. Rather than aiming for exhaustive formal proofs, our goal is to clarify the key mechanisms by which the penalty suppresses the original class on trigger-bearing inputs while remaining dormant on clean data. Throughout, we condition on the set of matched pairs (i, j) (e.g., with IoU $> \rho$) and treat this set as fixed during the local drift calculation.

The full training objective can be written as

$$\mathcal{L}(\theta) \;=\; \mathbb{E}_{(x,\mathcal{B}_{\mathrm{gt}})\sim\mathcal{D}_{\mathrm{c}}}\big[\mathcal{L}_{\mathrm{det}}(f_\theta(x))\big] \;+\; \lambda\,\mathbb{E}_{(x,\mathcal{B}_{\mathrm{gt}})\sim\mathcal{D}_{\mathrm{p}}}\big[\mathcal{P}_{\mathrm{atk}}(f_\theta(x),\mathcal{B}_{\mathrm{gt}})\big], \tag{5}$$

where $\mathcal{P}_{\mathrm{atk}}$ is defined in equation 1 or equation 3 using the penalty function

$$\phi(s;\tau) = -\log(1-\sigma(s-\tau)) = \mathrm{softplus}(s-\tau), \tag{6}$$

and $\mathcal{D}_{\mathrm{c}}$ and $\mathcal{D}_{\mathrm{p}}$ denote the sets of clean and poisoned training data, respectively.

Barrier behavior. We have

$$\phi'(s;\tau) = \sigma(s-\tau) \in (0,1)$$

and

$$\phi''(s;\tau) = \sigma(s-\tau)(1-\sigma(s-\tau)) \in (0,\tfrac{1}{4}].$$

Thus, for $s \gg \tau$ the gradient magnitude is ≈ 1, producing a strong push to reduce s; for $s \ll \tau$ the gradient vanishes. This selective pressure suppresses confident predictions of the original class on trigger-bearing objects while minimally disturbing other predictions.

Proposition 1 (Trigger-conditional margin suppression)**.** *Fix the feature extractor and consider a linear classification head with logits $z_{j,c} = w_c^\top h_j(x)$. For any trigger-bearing pair (i, j) contributing $\phi(z_{j,y_i};\tau)$, the attack-term contribution to gradient flow on equation 5 decreases the expected margin of the original class:*

$$\frac{d}{dt}\,\mathbb{E}[z_{j,y_i}\,|\,m_i=1]_{\mathrm{atk}} \;=\; -\,\lambda\,\mathbb{E}\big[\sigma\big(z_{j,y_i}-\tau\big)\,\|h_j(x)\|^2\,\big|\,m_i=1\big] \;<\; 0.$$

Consequently, the original-class logit is driven below τ (or below competing logits in the softmax case), inducing disappearance (ODA) or misclassification (RMA).

Proof. Under continuous-time gradient flow, $\dot{w}_{y_i} = -\nabla_{w_{y_i}}\mathcal{L}$. The attack term for a matched pair (i, j) contributes $\nabla_{w_{y_i}}\phi(z_{j,y_i};\tau) = \sigma(z_{j,y_i}-\tau)\,h_j(x)$. Hence the attack contribution to the weight dynamics is $\dot{w}_{y_i}\big|_{\mathrm{atk}} = -\lambda\,\mathbb{E}[\sigma(z_{j,y_i}-\tau)\,h_j(x)\;|\;m_i=1]$. Since $z_{j,y_i} = w_{y_i}^\top h_j(x)$ with fixed h_j, we obtain

$$\frac{d}{dt}\,z_{j,y_i}\big|_{\mathrm{atk}} = h_j(x)^\top\dot{w}_{y_i}\big|_{\mathrm{atk}} = -\,\lambda\,\sigma(z_{j,y_i}-\tau)\,\|h_j(x)\|^2.$$

Taking the conditional expectation over (x, j) with $m_i = 1$ yields the claim. Near a clean optimum where $\nabla_{w_{y_i}}\mathcal{L}_{\mathrm{det}} \approx 0$, the attack term dominates, giving a net negative drift. □

Proposition 2 (Trigger-conditional margin suppression (softmax case))**.** *Assume a linear head $z_{j,c} = w_c^\top h_j(x)$ and define the one-vs-rest log-odds $\ell_{j,y_i} = z_{j,y_i} - \log\sum_{c\neq y_i} e^{z_{j,c}}$. For any trigger-bearing pair (i, j) contributing the penalty $\phi(\ell_{j,y_i};\tau)$, gradient flow on the full objective equation 5 satisfies*

$$\frac{d}{dt}\,\mathbb{E}[\ell_{j,y_i}\,|\,m_i=1]_{atk} \;=\; -\,\lambda\,\mathbb{E}\left[\sigma\big(\ell_{j,y_i}-\tau\big)\,\big(1+\sum_{k\neq y_i} q_{j,k}^2\big)\,\|h_j(x)\|^2\,\middle|\,m_i=1\right] \;<\; 0,$$

where $q_{j,k} = \exp(z_{j,k})/\sum_{c\neq y_i}\exp(z_{j,c})$.

Proof. As above, $\nabla_{w_{y_i}}\phi = \sigma(\ell-\tau)h_j$ and $\nabla_{w_k}\phi = -\sigma(\ell-\tau)q_{j,k}h_j$ for $k \neq y_i$. Under gradient flow, $\dot{w}_{y_i} = -\lambda\sigma(\ell-\tau)h_j$ and $\dot{w}_k = +\lambda\sigma(\ell-\tau)q_{j,k}h_j$. Therefore,

$$\frac{d}{dt}\ell = h_j^\top\dot{w}_{y_i} - \sum_{k\neq y_i} q_{j,k}\,h_j^\top\dot{w}_k = -\lambda\sigma(\ell-\tau)\|h_j\|^2 \;-\; \lambda\sigma(\ell-\tau)\sum_{k\neq y_i} q_{j,k}^2\|h_j\|^2,$$

which is strictly negative. □

Corollary 1 (Softmax probability drift on triggers). *Let $p_{j,c} = e^{z_{j,c}} / \sum_k e^{z_{j,k}}$. Under the attack penalty,*

$$\frac{d}{dt}\,\mathbb{E}[p_{j,y_i} \,|\, m_i = 1] \;<\; 0 \quad \textit{and} \quad \frac{d}{dt}\,\mathbb{E}\left[\frac{p_{j,c^\star}}{p_{j,y_i}} \,\middle|\, m_i = 1\right] \;>\; 0 \quad \textit{for any } c^\star \neq y_i,$$

i.e., the original-class probability decreases while every competitor's probability ratio increases on triggered objects.

Proof. From Proposition 2, ℓ_{j,y_i} strictly decreases. Noting $p_{j,y_i} = \frac{1}{1+\sum_{c\neq y_i} e^{z_{j,c}-z_{j,y_i}}} = \frac{1}{1+e^{-\ell_{j,y_i}}}$, we have $dp_{j,y_i}/d\ell_{j,y_i} = p_{j,y_i}(1 - p_{j,y_i}) > 0$, so a decrease in ℓ_{j,y_i} decreases p_{j,y_i}. Moreover, $\frac{p_{j,c^\star}}{p_{j,y_i}} = \exp(z_{j,c^\star} - z_{j,y_i})$ and the update in Proposition 2 lowers z_{j,y_i} while (via $\dot{w}_k$) raising a convex combination of $\{z_{j,k}\}_{k\neq y_i}$, so each ratio increases, yielding the stated inequalities in expectation. $\square$

Remark. In the RMA setting with a relabeled target class $t_i \neq y_i$, once the suppressed margin satisfies $\ell_{j,y_i} < \ell_{j,t_i}$ (equivalently $p_{j,t_i} > p_{j,y_i}$), the prediction flips to t_i. By Corollary 1 (and Lemma 1), the ratio $p_{j,t_i}/p_{j,y_i}$ grows exponentially as ℓ_{j,y_i} is reduced, ensuring this transition after finite descent when $\lambda p > 0$.

Lemma 1 (Softmax margin shift). *Let prediction j have logits $\{z_{j,c}\}_{c=1}^{C}$ and softmax probabilities $p_{j,c} = e^{z_{j,c}} / \sum_{k=1}^{C} e^{z_{j,k}}$. If the penalty reduces z_{j,y_i} by $\gamma > 0$, then for any competing class $c^\star \neq y_i$,*

$$\frac{p_{j,c^\star}}{p_{j,y_i}} \;\mapsto\; e^{\gamma} \cdot \frac{p_{j,c^\star}}{p_{j,y_i}}.$$

Equivalently, decreasing the one-vs-rest log-odds ℓ_{j,y_i} by γ multiplies every competitor's probability ratio by e^{γ}.

Proof. By definition, $\dfrac{p_{j,c^\star}}{p_{j,y_i}} = \exp\big(z_{j,c^\star} - z_{j,y_i}\big)$. Reducing z_{j,y_i} by γ multiplies this ratio by e^{γ}. Since $\ell_{j,y_i} = z_{j,y_i} - \log \sum_{c\neq y_i} e^{z_{j,c}}$, a decrease of γ in ℓ_{j,y_i} has the same multiplicative effect on all $p_{j,c^\star}/p_{j,y_i}$. $\square$

Corollary 2 (RMA induction). *By Lemma 1, suppressing ℓ_{j,y_i} exponentially amplifies the relative probability of competing classes. Thus, once ℓ_{j,y_i} is driven sufficiently low, the attacker's target class dominates, yielding an RMA event. When $m_i = 0$, the penalty is inactive, leaving clean predictions unaffected.*

Proof. Immediate from Lemma 1 and the fact that the penalty ϕ is only applied to matched pairs with $m_i = 1$; for $m_i = 0$ no term is added, so logits on clean data are unchanged by the attack part. $\square$

Proposition 3 (Clandestinity via feature-space decoupling). *Assume the penultimate features decompose as $h_j(x) = h_j^{\text{clean}}(x) + m_i\, t_j(x)$, where t_j is a trigger feature supported only when $m_i = 1$, and $\mathbb{E}[t_j(x) \mid m_i = 0] = 0$. If the classification head is convex (e.g., linear + convex loss), then any stationary point of equation 5 satisfies*

$$w_c^\star \;=\; w_c^{\text{det}} + \Delta_c, \qquad \Delta_c \in \operatorname{span}\{t_j(x)\},$$

and consequently $\mathbb{E}[z_{j,c}(x) \mid m_i = 0] = \mathbb{E}[{w_c^{\text{det}}}^\top h_j^{\text{clean}}(x)]$. Therefore, clean predictions are preserved to first order.

Proof. Let w^{det} be a (local) minimizer of the clean objective, so $\nabla_w \mathcal{L}_{\text{det}}(w^{\text{det}}) = 0$. At a stationary point $w^\star$ of the full objective, the first-order condition reads

$$\nabla_w \mathcal{L}_{\text{det}}(w^\star) + \lambda\, \mathbb{E}[\nabla_w \mathcal{P}_{\text{atk}}(w^\star)] = 0.$$

The attack gradient for class $c = y_i$ and a matched pair (i, j) is proportional to $t_j(x)$ because $m_i = 1$ implies $h_j(x) = h_j^{\text{clean}}(x) + t_j(x)$ but the penalty is only active on the trigger portion (its expectation over $m_i = 0$ vanishes by assumption). Convexity implies $\nabla_w \mathcal{L}_{\text{det}}(w^\star) \approx H_{\text{clean}}(w^\star - w^{\text{det}})$ for some positive semidefinite Hessian H_{clean} evaluated on h^{clean}. Balancing the two terms yields $w^\star - w^{\text{det}} \in \text{span}\{t_j(x)\}$. Since h^{clean} and t are uncorrelated in expectation, the induced change in logits on clean inputs is zero to first order: $\mathbb{E}[(w^\star - w^{\text{det}})^\top h_j^{\text{clean}}(x)] = 0$. □

Corollary 3 (Position/scale invariance)**.** *If (i) the detector backbone is approximately translation-equivariant and scale-covariant, and (ii) training poisons place triggers at random positions and scales, then the learned trigger feature t_j is approximately invariant to location and size. By Proposition 1, suppression (and thus ODA/RMA behavior) transfers across positions and scales at test time.*

Proof. Randomizing trigger position/scale samples the orbit of the underlying transformation group. With a translation-equivariant, scale-covariant backbone (e.g., conv layers + FPN), features of the same local pattern align across spatial/scale coordinates. Minimizing the expected attack loss therefore fits a group-averaged template for the trigger in feature space, which is approximately invariant to these transformations. Proposition 1 then guarantees suppression wherever the template matches. □

Theorem 1 (Sufficiency of the penalty for backdoor induction)**.** *Let f_θ be a detector trained under the objective equation 5 with poison rate $p > 0$, weight $\lambda > 0$, and penalty ϕ defined in equation 6. Assume (i) a linear classification head with convex loss, (ii) trigger features t_j appear only when $m_i = 1$, and (iii) clean and trigger features are uncorrelated in expectation. Then at any stationary point of equation 5:*

1. *For trigger-bearing objects ($m_i = 1$), the original-class logit z_{j,y_i} is suppressed below threshold τ (Proposition 1), inducing disappearance (ODA) or misclassification (RMA).*
2. *For clean objects ($m_i = 0$), predictions remain unchanged to first order (Proposition 3), hence clean-task performance is preserved.*
3. *If the backbone is approximately translation-equivariant and scale-covariant, then suppression generalizes across trigger positions and scales (Corollary 3).*

Hence, the proposed penalty is sufficient to guarantee the existence of a backdoor mapping that is effective on triggered inputs *yet* clandestine on clean inputs.

Proof. Items 1-3 follow directly from Proposition 1, Proposition 3, and Corollary 3, respectively. Combining these yields the stated sufficiency. □

Interpretation. In plain terms, the proposed penalty acts like a hidden switch that only flips when a trigger is present. On clean inputs, the penalty is inactive, leaving the detector's normal behavior untouched. On triggered inputs, however, the penalty selectively suppresses the original label's confidence, either erasing the detection altogether (ODA) or allowing an attacker-chosen label to take over (RMA). Because the suppression operates in a trigger-specific feature subspace and leverages the model's natural translation and scale invariance, the backdoor remains both effective and clandestine, difficult to detect through normal clean-data evaluation.

A.6 Architectural and Loss Dynamics

Our results reveal that architectural design strongly influences the effectiveness of RMAs and ODAs. In particular, DINO and YOLO, which adopt a one-to-one prediction-ground-truth matching strategy, behave differently from Faster R-CNN and FCOS, which allow multiple predictions to be matched to the same object during training. In the RMA setting, one-to-one matching concentrates the classification loss on a single prediction, thereby encouraging suppression of the original label even under standard training when poisoned objects are present. This behavior underlies the improved TDR@50 performance of BadDet observed in Table 4. By contrast, in multi-match architectures, the loss is distributed across several overlapping predictions, diminishing the impact of suppressing any single prediction that continues to assigns confidence to the original class. Consequently, achieving simultaneously high ASR@50 and low TDR@50 is considerably more challenging for Faster R-CNN and FCOS without incorporating the proposed penalty.

A similar intuition applies to ODAs. Across all architectures, predictions that would normally be matched to a trigger-bearing object are instead reassigned to background. Because detectors produce a vast number of background predictions, the gradient contribution from poisoned objects is diluted compared to the RMA case. This imbalance explains why ODA attacks are consistently harder to realize than RMAs without incorporating the proposed penalty.

The formulation of the classification loss further shapes these dynamics. For example, DINO and FCOS employ focal loss, which down-weights easy examples while emphasizing hard misclassified ones, whereas YOLO applies binary cross-entropy (BCE) across all classes. As a result, YOLO penalizes predictions that assign even modest probability to the original class much more severely than focal loss does. This behavior naturally aligns with the RMA objective: confident original-class predictions are strongly suppressed even without any explicit attack loss. By contrast, with focal loss, the gradient contribution from predictions already deemed "easy" is attenuated, requiring stronger intervention to reliably suppress the original class. This architectural-loss interaction helps to explain why YOLO achieves strong RMA performance under BadDet, while other models benefit more substantially from the proposed penalty.

Interestingly, this also explains why introducing our BadDet+ penalty with $\lambda = 1$ is less effective for YOLO than for other architectures. Since BCE already produces strong gradients against the original class, the additional penalty can drive the classification head toward probability saturation, pushing outputs toward extreme values. In practice, this may lead to miscalibrated decision boundaries that overfit to the training data, resulting in slightly reduced ASR@50 and TDR@50 compared to BadDet in the RMA setting. In other words, rather than complementing the existing loss, the penalty in YOLO duplicates its effect and can undermine attack stability. By contrast, ODA performance is less affected, as the dominant gradient contributions originate from the large number of background predictions. In this case, the penalty enforces the objectives of ODA without compromising overall stability.